CU Journal of Non-Linear Fluid Mechanics
Vol. 01, No. 01, 2025
https://doi.org/10.11615/cujnlfm.01101-1

Study of chaos in Rayleigh-Bénard convection of water-alumina nanofluid with heat source/sink

Kanchana C. *[a] and D. Laroze[a]

[a] Instituto de Alta Investigación, Universidad de Tarapacá, Casilla 7 D, Arica 1000000, Chile

Abstract

Study of chaos in Rayleigh-Bénard convection of water-alumina nanofluid with internal heat source/sink is considered in the paper. A generalized Buongiorno two-phase model is used under the assumption of Boussinesq approximation and small-scale convective motion to formulate the governing equations for the nanofluid. By considering a minimal-mode Fourier representation, we arrive at the penta-model generalized Lorenz model. The largest Lyapunov exponent and the Kaplan-Yorke dimension are used to capture information on the commencement of chaos, windows of chaotic motion and periodic orbits. Suppression/inhibition of chaos due to presence of nanoparticles and heat source/sink are discussed. The study on linear stability is made for completeness. The present investigation reveals that the onset of chaos can be delayed using nanoparticles in the working medium. A further delay of chaos is possible by having a heat sink in the fluid layer. Thus the presence of nanoparticles in the fluid medium together with the internal heat sink leads to a long-term stable periodic orbit.

Keywords: Chaos; Heat source/sink; Lorenz model; Nanofluid.

1 Introduction

Nanofluids are mixtures of any base conventional fluid (hereinafter called as basefluid) with well-dispersed nano-sized particles (hereinafter called as nanoparticles). Research reports suggest that Masuda et al. [1] found such fluids. The term nanofluid was coined by Choi [2]. The choice of basefluids and nanoparticles is based on the application where it is being put to use. Nanofluids in heat transfer applications are now emerging spectacularly due to attention-grabbing features of nanoparticles such as high thermal conductivity, large surface area, stable suspensions without settling of particles, low abrasion, low/no clogging, low pressure loss and high heat transfer efficiency.

Many models are available in the literature to study the nanofluid based convection. These models have their own advantages and disadvantages for example, the single-phase model proposed by Khanafer et al. [3] incorporates the thermophysical properties of a nanofluid at static condition. This model is engineered under the assumption that nanoparticles and base fluid are chemically inert. The same time, the two-phase model proposed by Buongiorno [4] allows a relative velocity between the nanoparticles and the basefluid. Siddheshwar et al. [5] generalized the Buongiorno two-phase model by

* ckanchana@academicos.uta.cl

incorporating thermophysical properties of nanoliquids into the governing conservation equations. Thus, the generalized Buongiorno two-phase model consists of a two-component four-equation nonhomogeneous equilibrium model for mass, momentum, heat and nanoparticle transports.

Studies on controlling chaos in nanofluids concerning heat transfer applications are limited. Using a single-phase model, Jawdat et al. [6] showed inhibition of chaos in Rayleigh–Benard convection due to suspension of metal/metallic nanoparticles in water. Bhardwaj and Das [7] showed that chaos can be significantly controlled by tuning an applied magnetic field to regulate the Rayleigh number (a non-dimensional parameter that signifies the onset of convection). To arrive at this result, Bhardwaj and Das [7] considered Rayleigh–Benard convection in a water-copper-oxide nanofluid under the influence of a magnetic field. Using the single-phase description of Khanafer et al. [3], Kanchana et al. [8] made a comparative study of the effects of suspended multiwalled carbon nanotubes and alumina nanoparticles on the Rayleigh–Bénard convection in water and concluded that less expensive spherical alumina nanoparticles are preferable to more expensive multiwalled carbon nanotubes in heat transfer applications. Recently, Siddheshwar et al. [9] studied the dynamical behavior of the minimal and extended Lorenz models by considering water-copper and water-alumina nanofluids in the Rayleigh-Bénard convective system and showed that the extended penta-modal Lorenz system predicts advancement of onset of chaos when compared with that predicted by the classical third-order Lorenz model. Further, they reported that the individual influence of both nanoparticles in water is to advance the onset of chaos. Kanchana et al. [10] studied the influence of two-frequency rotational modulation on the dynamics of Rayleigh Bénard convection in water based nanoliquids and showed that there is no possibility of hyper chaos in the system for considered range of values of system parameters.

The presence of heat source/sink in the RBC problem is a regulatory mechanism to control heat transfer and chaos. It has applications in many areas. One such study is the Earth's mantle. The effect of internal heat generation on nonlinear Rayleigh-Bénard system was studied by Siddheshwar and Titus [11]. They showed that the effect of heat source/sink is to advance or delay the appearance of chaos. Linear and weakly nonlinear stability analyses of Rayleigh-Bénard convection with internal heat generation/absorption in water-based nanoliquids is studied analytically by Kanchana and Yi [12] using the generalized Buongiorno two-phase model. Meenakshi and Siddheshwar [13] studied the same problem using the single-phase model. They showed that the influence of heat generation/absorption is to augment/inhibit onset of convection and enhance/diminish heat transport. The linear and weakly nonlinear study of the effect of rotation and internal heat source/sink on Bénard convection was reported by Sanjalee et al. [14] using the modified Buongiorno model. They showed that the heat transfer rate increases by 22 % when the nanofluidic system is placed in the rotating frame of reference under the presence of an internal heat source. The influence of internal heat generation/absorption on various cases of natural convection is studied by Shivaraj et al. [15] and Yadav et al. [16].

The study on chaos in RBC in nanofluids with heat source/sink is very scarce. More recently, Sanjalee et al.[17] considered such a study under the effect of a non-uniform heat source in a hybrid Casson nanoliquid and observed significant advance in the onset of chaos when free-free and rigid-rigid boundaries were considered under the combined influence of the heat source and the nanoparticles.

In the present study, we have considered the RBC in a water-alumina nanofluid in the presence of a heat source/sink and reported about the combined influence these mechanisms have on the onset of chaos and on the periodic orbits. We consider a penta-modal Lorenz system for the study. We considered the generalized Buongiorno model proposed by Siddheshwar et al. [5] and arrived at the penta-modal Lorenz model. The largest Lyapunov exponent, using the algorithm proposed by Wolf et al. [18] and Kaplan-Yorke dimension [19]–[21], are used to characterize the chaotic and periodic behavior of the trajectories of the penta-modal system.

2 Mathematical formulation

The set-up of the problem considered is a horizontal layer of infinite extent with water/water-alumina nanofluid confined between the two parallel planes. If the height of the plane is h, and the width is b then $h \ll b$ is the considered extent of the layer. The upper and lower boundaries are assumed to be at constant temperatures T_0 and $T_0 + \Delta T$ with $\Delta T > 0$, and constant volumetric nanoparticle concentrations ϕ_0 and $\phi_0 + \Delta\phi$ with $(\Delta\phi > 0)$. As a regulatory mechanism, an uniform heat source/sink is assumed to exist. A schematic of the set-up is shown in Figure 1. With this aforementioned set-up, the

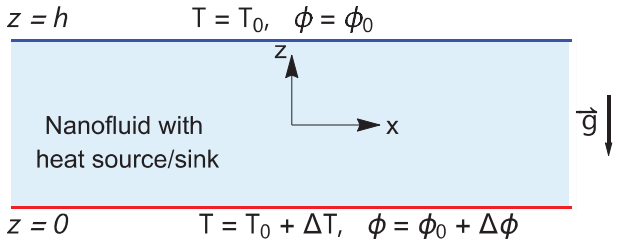

Figure 1: Physical configuration of the problem.

governing equations take the form:

$$\nabla \cdot \vec{q} = 0, \tag{1}$$

$$\rho \frac{\partial \vec{q}}{\partial t} = -\nabla p + \mu \nabla^2 \vec{q} + [\rho - (\rho\beta_1)(T - T_0) + (\rho\beta_2)(\phi - \phi_0)]\,\vec{g}, \tag{2}$$

$$(\rho c_p)\left[\frac{\partial T}{\partial t} + (\vec{q} \cdot \nabla)T\right] = k\nabla^2 T + Q(T - T_0), \tag{3}$$

$$\frac{\partial \phi}{\partial t} + (\vec{q} \cdot \nabla)\phi = D_B \nabla^2 \phi + \frac{D_T}{T_0}\nabla^2 T, \tag{4}$$

where $\vec{q} = (u, w)$ is the velocity vector in m/s, t is time in s, p is the pressure in Pa, $\vec{g} = (0, 0, -g)$, acceleration due to gravity in m/s^2, T is the temperature in K, μ, ρ, β_1, β_2 and α respectively represent dynamic viscosity (in kg/ms), density (in kg/m^2), thermal expansion coefficient (in $1/K$), concentration analogy of thermal expansion coefficient (in $1/Kg$) and thermal diffusivity (in m^2/s) and these quantities represent the nanofluid properties, which are calculated using the properties of water and alumina nanoparticles as shown in Table 1.

Models	**Quantities**
Hamilton-Crosser model [22]	$\dfrac{k}{k_{bl}} = \dfrac{\left(\frac{k_{np}}{k_{bl}} + 2\right) - 2\chi\left(1 - \frac{k_{np}}{k_{bl}}\right)}{\left(\frac{k_{np}}{k_{bl}} + 2\right) + \chi\left(1 - \frac{k_{np}}{k_{bl}}\right)}$
Brinkman model [23]	$\dfrac{\mu}{\mu_{bl}} = \dfrac{1}{(1-\chi)^{2.5}}$
Traditional mixture theory	$(\rho \mathtt{C}_p) = (\rho \mathtt{C}_p)_{bl}(1-\chi) + \chi(\rho \mathtt{C}_p)_{np}$, $(\rho\beta) = (\rho\beta)_{bl}(1-\chi) + \chi(\rho\beta)_{np}$, $\rho_{nl} = \rho_{bl}(1-\chi) + \chi\rho_{np}$ $\mathtt{C}_p = \dfrac{(\rho \mathtt{C}_p)}{\rho}$, $\beta = \dfrac{(\rho\beta)}{\rho}$, $\alpha_{nl} = \dfrac{k}{(\rho \mathtt{C}_p)}$

Table 1: Models for determining thermophysical properties of nanofluids.

The quantities D_B and D_T are the diffusion coefficients and are defined as

$$D_B = \frac{K_B T_0}{3\pi\mu d_{np}} \text{ and } D_T = 0.26\frac{k}{2k + k_{np}}\frac{\mu}{\rho}\chi,$$

where χ denotes the alumina nanoparticle volume fraction and is calculated as

$$\chi = \frac{\text{Volume fraction of alumina}}{\text{Volume fraction of (alumina+water)}}.$$

While writing the governing equations (1) - (4), we assumed the following:

- All physical quantities are independent of the horizontal coordinate and hence the considered structure of the cells are rolls.
- It is assumed that the density is constant in all terms in Eq. (2) except the body force, where it is function of temperature. We thereby imply the assumption of the Oberbeck-Boussinesq approximation.
- In writing Eq. (2), we ignore the $(\vec{q} \cdot \nabla)\vec{q}$ term. Thereby, we mean that only a small-scale convective motion is considered.

- Alumina nanoparticles are assumed to be uniform in size, spherical in shape and well dispersed in water.
- Alumina nanoparticles and water particles are assumed to be in thermal equilibrium locally.
- The horizontal boundaries are assumed to be stress-free, isothermal and iso-nanoparticle concentration and are written as :

$$\left.\begin{aligned} u=0, w=0, \frac{\partial u}{\partial z}+\frac{\partial w}{\partial x}=0, T=T_0+\triangle T, \phi=\phi_0+\triangle\phi \text{ at } z=0 \\ u=0, w=0, \frac{\partial u}{\partial z}+\frac{\partial w}{\partial x}=0, T=T_0,\ \phi=\phi_0 \text{ at } z=h \end{aligned}\right\}. \tag{5}$$

- There is a relative velocity between water and alumina nanoparticles.
- The effect of Brownian motion is negligibly small ([24], [5]).

All these mentioned assumptions are made for the purpose of making the study theoretically manageable, and based on previous investigations these assumptions are valid.

At the motionless basic state the governing equations (1)-(4) subject to the boundary conditions (5) have the following solution:

$$\vec{q}_b=\vec{0}, \tag{6}$$

$$p_b=-\int\left[\rho_0+(\rho\beta_2)_{nl}\left(1-\frac{z}{h}\right)\left(\Delta\phi+\frac{D_T\Delta T}{T_0D_B}\right)-(\rho\beta_1)_{nl}\Delta T f\left(\frac{z}{h}\right)\right.$$
$$\left.-(\rho\beta_2)_{nl}\frac{D_T\Delta T}{D_BT_0}f\left(\frac{z}{h}\right)\right]dz+C^*, \tag{7}$$

$$T_b=T_0+\Delta T f\left(\frac{z}{h}\right), \tag{8}$$

$$\phi_b=\phi_0+\left(1-\frac{z}{h}\right)\left(\Delta\phi+\frac{D_T\Delta T}{T_0D_B}\right)-\frac{D_T\Delta T}{D_BT_0}f\left(\frac{z}{h}\right), \tag{9}$$

where the subscript b denotes the basic state solution, $f\left(\frac{z}{h}\right)=\frac{\sin\left(\sqrt{Ra_I}\left(1-\frac{z}{h}\right)\right)}{\sin\sqrt{Ra_I}}$, $Ra_I=\frac{Qh^2}{\alpha_{nl}}$ is the internal Rayleigh number and C^* is an integration constant.
Applying a small thermal perturbation to the system results in

$$\vec{q} = \vec{q}', \tag{10}$$

$$p = -\int\left[\rho_0+(\rho\beta_2)_{nl}\left(1-\frac{z}{h}\right)\left(\Delta\phi+\frac{D_T\Delta T}{T_0D_B}\right)\right.$$
$$\left.-(\rho\beta_1)_{nl}\Delta T f\left(\frac{z}{h}\right)-(\rho\beta_2)_{nl}\frac{D_T\Delta T}{D_BT_0}f\left(\frac{z}{h}\right)\right]dz+C^*+p', \tag{11}$$

$$T = T_0+\Delta T f\left(\frac{z}{h}\right)+T', \tag{12}$$

$$\phi = \phi_0+\left(1-\frac{z}{h}\right)\left(\Delta\phi+\frac{D_T\Delta T}{T_0D_B}\right)-\frac{D_T\Delta T}{D_BT_0}f\left(\frac{z}{h}\right)+\phi', \tag{13}$$

where the prime denotes perturbation. The primed quantities are considered to be infinitesimal in the case of a linear stability analysis and finite when a weakly nonlinear stability analysis is performed.

Substituting the expressions (10)-(13) in Eqs. (1) - (4), we obtain the governing equations in component form as follows:

$$\frac{\partial u'}{\partial x}+\frac{\partial w'}{\partial z} = 0, \tag{14}$$

$$\rho\frac{\partial u'}{\partial t} = -\frac{\partial p'}{\partial x}+\mu\nabla^2 u', \tag{15}$$

$$\rho\frac{\partial w'}{\partial t} = -\frac{\partial p'}{\partial z}+\mu\nabla^2 w'+(\rho\beta_1)_{nl}T'g-(\rho\beta_2)\phi' g, \tag{16}$$

$$\frac{\partial T'}{\partial t} = \alpha_{nl}\nabla^2 T'+QT'-w'\frac{dT_b}{dz}-u'\frac{\partial T'}{\partial x}-w'\frac{\partial T'}{\partial z}, \tag{17}$$

$$\frac{\partial \phi'}{\partial t} = D_B\nabla^2\phi'+\frac{D_T}{T_0}\nabla^2 T'-w'\frac{d\phi_b}{dz}-u'\frac{\partial \phi}{\partial x}-w'\frac{\partial \phi}{\partial z}, \tag{18}$$

Eliminating the pressure term in Eqs. (15) and (16) and introducing the stream function, ψ, in the form:

$$u' = -\frac{\partial \psi}{\partial z},\quad w' = \frac{\partial \psi}{\partial x}, \tag{19}$$

we obtain the governing equations in the form :

$$\rho\frac{\partial}{\partial t}(\nabla^2\psi) = \mu_{nl}\nabla^4\psi+(\rho\beta_1)_{nl}\frac{\partial T'}{\partial x}g-(\rho\beta_2)_{nl}\frac{\partial \phi'}{\partial x}g, \tag{20}$$

$$\frac{\partial T'}{\partial t} = \alpha_{nl}\nabla^2 T'+QT'-\frac{\partial \psi}{\partial x}\frac{dT_b}{dz}-\frac{\partial \psi}{\partial x}\frac{\partial T'}{\partial z}+\frac{\partial \psi}{\partial z}\frac{\partial T'}{\partial x}, \tag{21}$$

$$\frac{\partial \phi'}{\partial t} = D_B\nabla^2\phi'+\frac{D_T}{T_0}\nabla^2 T'-\frac{\partial \psi}{\partial x}\frac{d\phi_b}{dz}-\frac{\partial \psi}{\partial x}\frac{\partial \phi'}{\partial z}+\frac{\partial \psi}{\partial z}\frac{\partial \phi'}{\partial x}. \tag{22}$$

Introducing the following non-dimensional variables

$$(x^*,z^*) = \left(\frac{x}{h},\frac{z}{h}\right),\quad t^* = \frac{\alpha_{bl}t}{h^2},\quad \Psi = \frac{\psi}{\alpha_{bl}},\Theta = \frac{T'}{\triangle T},\quad \Phi = \frac{\phi'}{\triangle\phi}\Bigg\}, \tag{23}$$

Eqs. (20)-(22) can be written in dimensionless form as (after neglecting the asterisk):

$$\frac{\partial}{\partial t}(\nabla^2\Psi) = Pr\left[a_1\nabla^4\Psi+a_1^2 Ra\frac{\partial\Theta}{\partial X}-a_1^2 Ra_\phi\frac{\partial\Phi}{\partial X}\right], \tag{24}$$

$$\begin{aligned}\frac{\partial\Theta}{\partial t} &= a_1\nabla^2\Theta+a_1 Ra_I\Theta+\frac{\sqrt{Ra_I}}{\sin\sqrt{Ra_I}}\cos(\sqrt{Ra_I}(1-Z))\frac{\partial\Psi}{\partial X}\\ &\quad -J(\Psi,\Theta),\end{aligned} \tag{25}$$

$$\begin{aligned}\frac{\partial\Phi}{\partial t} &= \frac{a_1}{Le}\nabla^2\Phi+\frac{a_1 N_A}{Le}\nabla^2\Theta+(1+N_A)\frac{\partial\Psi}{\partial X}-J(\Psi,\Phi)\\ &\quad -N_A\frac{\sqrt{Ra_I}}{\sin\sqrt{Ra_I}}\cos(\sqrt{Ra_I}(1-Z))\frac{\partial\Psi}{\partial X},\end{aligned} \tag{26}$$

The nondimensional parameters arising in Eqs. (24)-(26) are

$$\left.\begin{aligned} Pr = \frac{\mu}{\rho\alpha}(\text{ the Prandtl number}),\ a_1 = \frac{\alpha}{\alpha_{bl}}(\text{ the diffusivity ratio}),\\ Ra = \frac{(\rho\beta)\Delta T h^3 g}{\mu\alpha}(\text{ the thermal Rayleigh number}),\\ Ra_\phi = \frac{\mu_{bl}\ \alpha_{bl}(\rho_{np}-\rho)}{\mu\ \alpha(\rho_{np}-\rho_{bl}}Ra_{\phi_{bl}}(\text{ the concentration Rayleigh number}),\\ Le = \frac{\alpha\,\mu}{\alpha_{bl}\ \mu_{bl}}Le_{bl}(\text{ the Lewis number}),\ \text{and}\\ N_A = \frac{k(2k_{bl}+k_{np})}{k_{bl}(2k+k_{np})}\left(\frac{\mu}{\mu_{bl}}\right)^2\frac{\rho_{bl}}{\rho}N_{A_{bl}}(\text{ the modified diffusivity ratio}), \end{aligned}\right\}. \tag{27}$$

The terms $J(\Psi,\Theta)$ and $J(\Psi,\Phi)$ are defined as Jacobians.

The boundary condition now takes the form:

$$\Psi = \nabla^2\Psi = \Theta = \Phi = 0 \text{ at } z = 0,1. \tag{28}$$

Using the minimal mode Fourier representation, we next make a weakly nonlinear stability analysis and arrive at the generalized Lorenz model.

2.1 Derivation of the generalized penta-modal Lorenz model

We perform a weakly nonlinear stability analysis by considering the minimal Fourier representation for the stream function, temperature, and nanoparticle concentration as follows:

$$\Psi(x,y,t) = \frac{\sqrt{2}a_1\delta^2}{\pi^2\kappa_c}X(t)g_1(x,z), \tag{29}$$

$$\Theta(x,y,t) = \frac{\sqrt{2}}{\pi r}Y(t)g_2(x,z) - \frac{1}{\pi r}Z(t)g_3(x,z), \tag{30}$$

$$\Phi(x,y,t) = \frac{\sqrt{2}}{\pi}L(t)g_2(x,z) + \frac{1}{\pi}M(t)g_3(x,z), \tag{31}$$

where $r = \dfrac{Ra\kappa_c^2\pi^2}{\delta^6}$, $\delta^2 = \pi^2(1+\kappa_c^2)$ and $X(t), Y(t), Z(t), L(t)$ and $M(t)$ are the amplitudes and g_i's are given by:

$$g_1(x,z) = \sin(\pi\kappa_c x)\sin(\pi z), \tag{32}$$

$$g_2(x,z) = \cos(\pi\kappa_c x)\sin(\pi z), \tag{33}$$

$$g_3(x,z) = \sin(2\pi z). \tag{34}$$

Now substituting Eqs. (29)-(31) in Eqs. (24)-(26), multiplying the resulting equations by their respective eigenfunctions as mentioned in Eq. (32)-(34) and integrating over a pair of rotating and counter-rotating Rayleigh-Bénard cells, i.e., one wave-length, we

obtain the penta-modal Lorenz model:

$$\frac{dX}{d\tau} = Pr\, a_1 \left[-X + Y - r_\phi L\right], \tag{35}$$

$$\frac{dY}{d\tau} = a_1 \left[r\left(\frac{1}{1-r_I'}\right)X - Y(1-Ra_I') - XZ\right], \tag{36}$$

$$\frac{dZ}{d\tau} = a_1 \left[-b_1 Z(1-r_I') + XY\right], \tag{37}$$

$$\frac{dL}{d\tau} = a_1 \left[\left(1 - \frac{N_A r_I'}{1-r_I'}\right)X - \frac{N_A}{rLe}Y - \frac{1}{Le}L + XM\right], \tag{38}$$

$$\frac{dM}{d\tau} = a_1 \left[\frac{b_1 N_A}{rLe}Z - \frac{b_1}{Le}M - XL\right], \tag{39}$$

where $\tau = \delta^2 t$, $r_\phi = \dfrac{Ra_\phi \kappa_c^2 \pi^2}{\delta^6}$, $Ra_I' = \dfrac{Ra_I}{\delta^2}$, $r_I' = \dfrac{Ra_I}{4\pi^2}$ and $b_1 = \dfrac{4\pi^2}{\delta^2}$.

The penta-modal Lorenz model is invariant under the following transformation:

$$(X, Y, Z, L, M) \longrightarrow (-X, -Y, Z, -L, M). \tag{40}$$

Further,

$$\begin{aligned} &\frac{d}{dX}\left(\frac{dX}{d\tau}\right) + \frac{d}{dY}\left(\frac{dY}{d\tau}\right) + \frac{d}{dZ}\left(\frac{dZ}{d\tau}\right) + \frac{d}{dL}\left(\frac{dL}{d\tau}\right) + \frac{d}{dM}\left(\frac{dM}{d\tau}\right) \\ &= -\frac{a_1}{Le}\left[1 + b_1 + Le(Pr - (Ra_I + r_I) + 2)\right] \\ &< 0 \quad \text{since } a_1, Le, b_1, Pr > 0 \text{ and } (Ra_I + r_I) < Pr + 2. \end{aligned} \tag{41}$$

Thus, we note that the penta-modal Lorenz model retains features of the classical Lorenz model, viz., symmetry and dissipative nature.

3 Results and discussion

Study of regular convection, chaos and periodic motion in RBC of water-alumina nanofluid in the presence of heat source/sink is considered in the paper. The choice of nanoparticles was made based on the feasibility study reported by Kanchana et al. [8] which showed many advantages of these choices over other nanoparticles. The thermophysical properties of alumina nanoparticles and water base fluid at $300^0 K$ are recorded in Table 2.

Using Table 1 and the thermophysical properties of water and alumina nanoparticles documented in Table 2, we have calculated the thermophysical properties of water-alumina nanofluid by taking $\chi = 0.04$. It is to be noted that the value of χ is maintained to be 0.04 throughout the paper. Further, following the definition of the nondimensional parameters mentioned in Eq. (27), the values for Pr, Ra_ϕ, Le and N_A are found by calculation to be $Ra_{\phi\, bl} = 4$, $Le_{bl} = 2$ and $N_{A\, bl} = 4$ and these recorded in Table 3.

Material	**Density**	**Thermal Conductivity**	**Specific heat**	**Thermal expansion coefficient**
Water	997	0.613	4179	21×10^{-5}
Alumina	3970	46	765	0.85×10^{-5}
Water-alumina	1115.92	0.687	3693.17	18.13×10^{-5}

Table 2: Thermophysical properties of various materials at $300^0 K$ [25]. For calculating the thermophysical properties of water-alumina nanofluid the value of χ is taken to be 0.04.

Pr	Ra_ϕ	Le	N_A
5.30221	3.06253	2.51883	4.92846

Table 3: Thermophysical properties of water-alumina nanofluid calculated for $\chi = 0.04$.

A linear stability analysis reveals that

$$\frac{Ra}{(1-Ra_I)(1-r_I)} = F\left(\frac{Ra_w}{(1-Ra_I)(1-r_I)}\right), \tag{42}$$

where F is a factor that gives the ratio of the critical Rayleigh number values of the water-alumina nanofluid to that of water and is defined as:

$$F = \frac{(\rho\beta_1)_{nf}\alpha_w\mu_w}{\rho\beta_1\alpha\mu}. \tag{43}$$

Using Eq. (42), the values of the critical Rayleigh number of nanofluid and water are found. A comparison of these values for heat source and heat sink is made and depicted in the bar chart in Figure 2a. The bar chart in Figure 2b represents the corresponding critical wave number. These barcharts clearly indicate the advancement of convection due to the presence of alumina nanoparticles in water. Furthermore, a heat source promotes convection while heat sink dampens it. The influence of alumina nanoparticles in water is to increases the value of the critical wave number and thereby we see increased number of cells in nanofluids compared to that in water. However, the influence of the heat source/sink on the critical wave number is similar to that seen regarding its influence on the critical Rayleigh number.

Several metrics are used to characterize chaos[26]. One of them is the largest Lyapunov exponent(LLE) whose value indicates whether the attractor is a fixed point, a chaotic attractor, or a periodic orbit:

$$LLE \begin{cases} < 0, \text{ a fixed point} \\ = 0, \text{ a periodic orbit} \\ > 0, \text{ a chaotic or strange attractor} \end{cases} \tag{44}$$

To calculate the LLE we followed the algorithm proposed by Wolf et al. [18]. To solve the penta-modal Lorenz system, the classical fourth order Runge-Kutta method is

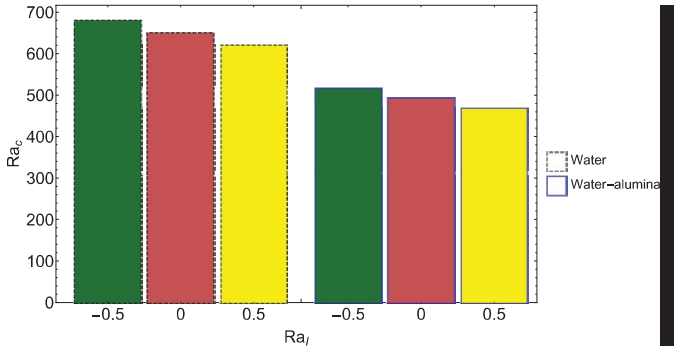

(a) The critical Rayleigh number values

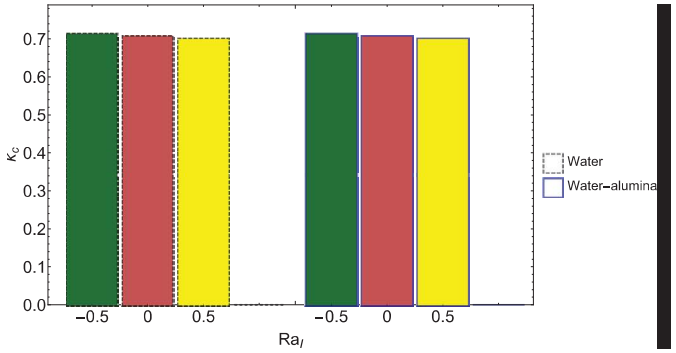

(b) The critical wave number values

Figure 2: Barchart of the values of critical Rayleigh number and wave number for different cases.

used with a time step of 0.005. Numerical simulation is performed for both water and water-alumina in the presence/absence of heat source/sink as shown in Figure 3.

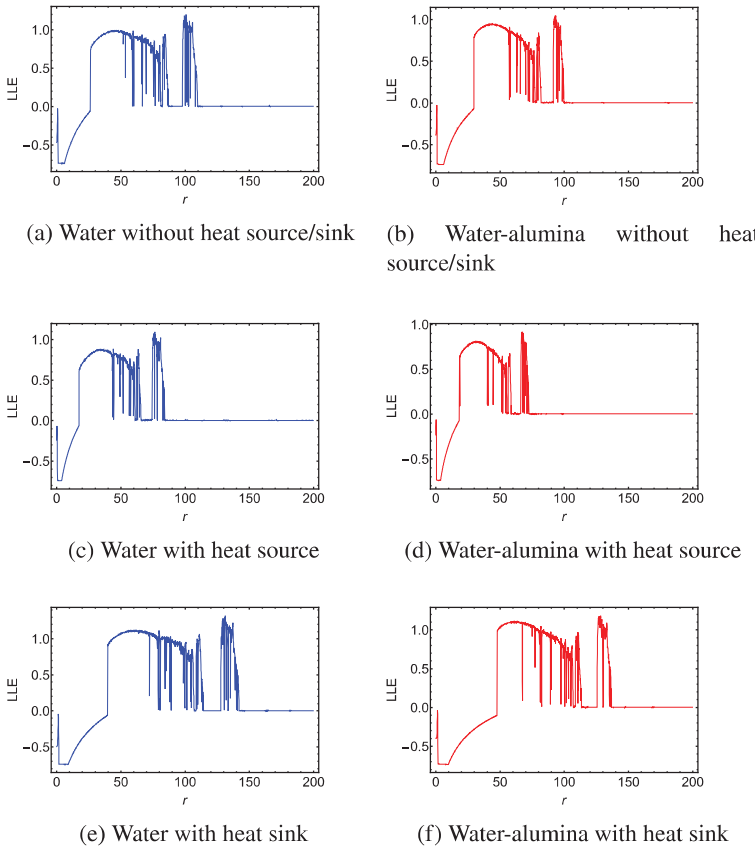

(a) Water without heat source/sink

(b) Water-alumina without heat source/sink

(c) Water with heat source

(d) Water-alumina with heat source

(e) Water with heat sink

(f) Water-alumina with heat sink

Figure 3: Plot of maximum Lyapunov exponent versus r for water and water-alumina nanofluids in the presence/absence of a heat source/sink.

Figure 3 clearly shows that the onset of chaos is delayed due to the presence of alumina nanoparticles in water. However, the effect of adding a uniform heat source leads to preponement of the onset while a heat sink postpones it. Having a heat source in the system provides energy to the system and hence this observation. An interesting observation is that the chaotic regime is suppressed due to the presence of alumina nanoparticle in water. This suppression is significant when a heat source is added. Thus, the suspension of nanoparticles in the base fluid and introduction of the heat source is a novel way of suppressing chaos and having long-term stability in the form of periodic orbits.

The barchart in Figure 4a reiterates the effects of heat source and heat sink on the onset of chaos in both water and water-alumina nanofluid. Further, at $r = r_H$, we have calculated the Kaplan-Yorke dimension (D_{KY}) using the procedure proposed by Kaplan and Yorke [19]–[21]. The value of D_{KY} signifies the nature of the system. For example, $D_{KY} = 0$ indicates a stable equilibrium point whereas, a non-integer D_{KY} value represents the chaotic attractor. The Table 4 and the barchart in Figure 4b clearly show that the D_{KY} is not an integer at $r = r_H$ indicating the onset of chaotic attractor at $r = r_H$. Further, these values are large for water-alumina nanofluid compared to that of water indicating post-ponement of the onset of chaos due to the presence of nanoparticles in water.

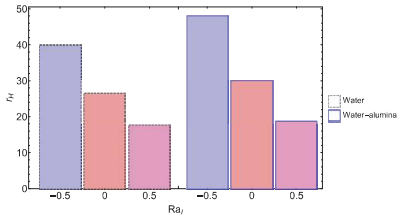

(a) The values of Hopf Rayleigh number

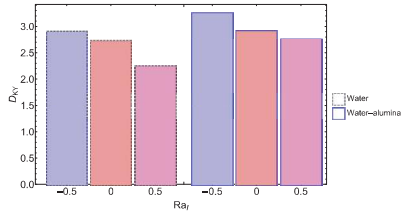

(b) The values of Kaplan-Yorke dimension

Figure 4: Barchart of values of Hopf Rayleigh number and Kaplan-Yorke dimension for different cases.

Working medium	Ra_I	Ra_c	κ_c	r_H	D_{KY}
Water	-0.5	680.6387	0.712994	39.9	2.90297
	0	649.5107	0.707107	26.5	2.73541
	0.5	618.8253	0.700897	17.7	2.24497
Water - alumina	-0.5	515.5348	0.712991	48	3.24688
	0	491.9576	0.707107	29.9	2.91603
	0.5	468.7156	0.7009	18.6	2.7584

Table 4: Values of Ra_c, κ_c, r_H and D_{KY} for different cases.

Final remark

There are many real world applications where chaotic and periodic motions can be seen, for example, in the case of liquid crystals, a tumbling or wagging motion of the director produces a periodic orbit in the rheological properties. Controlling chaotic motion and/or periodic motion is a challenging task when the chaos needs to be controlled without disturbing the physical nature of the set-up and the control is only intrinsic. The present work is one such theoretical experiment to control chaotic and periodic motions. The final remarks from the study are as follows:

1. Using nanoparticles in a working fluid medium, one can delay the onset of chaos.
2. An effective way of delaying the appearance of chaos is to have a heat sink in the system. A heat source advances the onset of chaos.
3. It is possible to have long-term stable periodic orbits in the system by opting nanofluid over base fluid as a working fluid medium.
4. One can favor chaos over periodic motion by considering a heat sink.

The above observations are for certain fixed value of non-dimensional parameters. It is not true for all values of the parameters. Furthermore, the dynamical system considered here is a penta-modal Lorenz model with the possibility of the hyper chaos. This forms the future scope of the study.

References

[1] Masuda H., Ebata A., Teramae K., and Hishinuma N., "Alteration of thermal conductivity and viscosity of liquid by dispersing ultra-fine particles. dispersion of Al_2O_3, SiO_2 and TiO_2 ultra-fine particles", *Netsu Bussei*, vol. 7, (4), 227—233, 1993.

[2] Choi S. U. S. and Eastman J. A., "Enhancing thermal conductivity of fluids with nanoparticles", *International Mechanical Engineering Congress & Exposition*, vol. 231, p. 31 109, 1995.

[3] Khanafer K., Vafai K., and Lightstone M., "Buoyancy-driven heat transfer enhancement in a two-dimensional enclosure utilizing nanofluids", *International Journal of Heat and Mass Transfer*, vol. 46, (19), 3639—3653, 2003.

[4] Buongiorno J., "Convective transport in nanofluids", *ASME Journal of Heat Transfer*, vol. 128, (3), pp. 240–250, 2006.

[5] Siddheshwar P. G., Kanchana C., Kakimoto Y., and Nakayama A., "Steady finite-amplitude Rayleigh–Bénard convection in nanoliquids using a two-phase model: Theoretical answer to the phenomenon of enhanced heat transfer", *ASME Journal of Heat Transfer*, vol. 139, (1), p. 012 402, 2017.

[6] Jawdat J. M., Hashim I., and Momani S., "Dynamical systems analysis of thermal convection in a horizontal layer of nanofluids heated from below", *Mathematical Problems in Engineering*, vol. 2012, pp. 1–13, 2012.

[7] Bhardwaj R. and Das S., *Industrial mathematics and complex systems: emerging mathematicals models, method and algorithms*. Springer Nature,Singapore, 2017.

[8] Kanchana C., Zhao Y., and Siddheshwar P. G., "A comparative study of individual influences of suspended multiwalled carbon nanotubes and alumina nanoparticles on Rayleigh–Bénard convection in water", *Physics of Fluids*, vol. 30, p. 084 141, 2018.

[9] Siddheshwar P. G., Idris R., Kanchana C., and Laroze D., "Rayleigh–Bénard convection of water-copper and water-alumina nanofluids based on minimal - and higher - mode Lorenz models", *International Journal of Bifurcation and Chaos*, vol. 33, p. 2 350 104, 2023.

[10] Kanchana C., Siddheshwar P. G., and Laroze D., "Influence of two-frequency rotational modulation on the dynamics of the Rayleigh–Bénard convection in water-based nanoliquids with either AA7072 or AA7075 nanoparticles", *International Journal of Bifurcation and Chaos*, vol. 34, p. 2 450 043, 2024.

[11] Siddheshwar P. G. and Titus P. S., "Nonlinear Rayleigh–Bénard convection with variable heat source", *ASME Journal of Heat Transfer*, vol. 135, p. 122 502, 2013.

[12] Kanchana C. and Yi Z., "Effect of internal heat generation/absorption on Rayleigh-Bénard convection in water well-dispersed with nanoparticles or carbon nanotubes", *International Journal of Heat and Mass Transfer*, vol. 127, pp. 1031–1047, 2018.

[13] Meenakshi N. and Siddheshwar P. G., "A theoretical study of enhanced heat transfer in nanoliquids with volumetric heat source", *Journal of Applied mathematics and Computing*, vol. 57, pp. 703–728, 2018.

[14] Sanjalee, Sharma Y. D., and Yadav O. P., "The linear and non-linear study of effect of rotation and internal heat source/sink on Bénard convection", *Fluid Dynamics Research*, vol. 55, p. 045 503, 2023.

[15] Shivaraj B., Siddheshwar P. G., and Uma D., "Effects of variable viscosity and internal heat generation on Rayleigh–Bénard convection in Newtonian dielectric liquid", *International Journal of Applied and Computational Mathematics*, vol. 7, p. 119, 2021.

[16] Yadav D., Mahabaleshwar U. S., Wakif A., and Chand R., "Significance of the inconstant viscosity and internal heat generation on the occurrence of Darcy-Brinkman convective motion in a couple-stress fluid saturated porous medium: An analytical solution", *International Communications in Heat and Mass Transfer*, vol. 122, p. 105 165, 2021.

[17] Sanjalee, Sharma Y. D., and Yadav O. P., "Regular and chaotic Bénard convection in hybrid casson nanoliquid under the effect of non-uniform heat source", *Chinese Journal of Physics*, vol. 83, pp. 28–50, 2023.

[18] Wolf A., Swift J. B., Swinney H. L., and Vastano J. A., "Determining Lyapunov exponents from a time series", *Physica D*, vol. 16, 285—317, 1985.

[19] Kaplan J. L. and Yorke J. A., *Chaotic behavior of multidimensional difference equations*. Springer, Germany, Berlin, 1979.

[20] Kaplan J. L. and Yorke J., "The onset of chaos in a fluid flow model of Lorenz", *Annals of the New York Academy of Sciences*, vol. 316, 400—407, 1979.

[21] Kaplan J. L. and Yorke J., "Preturbulence: A regime observed in a fluid flow model of Lorenz", *Communications in Mathematical Physics*, vol. 67, 93—108, 1979.

[22] Hamilton R. and Crosser O., "Thermal conductivity of heterogeneous two - component systems", *Industrial & Engineering Chemistry Fundamentals*, vol. 1, pp. 187–191, 1962.

[23] Brinkman H., "The viscosity of concentrated suspensions and solutions", *Journal of Chemical Physics*, vol. 20, p. 571, 1952.

[24] Tzou D., "Thermal instability of nanofluids in natural convection", *International Journal of Heat and Mass Transfer*, vol. 51, 2967–2979, 2008.

[25] Bergman T., Incropera F., DeWitt D., and Lavine A., *Fundamentals of Heat and Mass Transfer*. John Wiley & Sons, New York, 2011.

[26] Kanchana C., Siddheshwar P. G., and Laroze D., "Control of chaos and intermittent periodic motions in Rayleigh-Bénard convection using a feedback controller", *Nonlinear Dynamics*, vol. https://doi.org/10.1007/s11071-024-10494-1, 2024.

Acknowledgements

KC is grateful to the Universidad de Tarapacá(Chile) for supporting her research work. DL acknowledges partial financial support from Centers of Excellence with BASAL/ANID financing, Grant AFB220001, CEDENNA.

Data Availability

The data that support the findings of this study are available upon reasonable request.